The linear Paul Trap's Confined Stability Area for 40Ca+ Ions

Basem R. Kazem[1]   **Mezher B. Saleh[2]**

[1]*Department of Physics, College of Science, Al- Mustansiriyah University, Baghdad, Iraq.*
[2]*Department of Physics, College of Science, Al- Mustansiriyah University, Baghdad, Iraq.*
[1]***E-mail: basemraheem@uomustansiriyah.edu.iq***
[2]***E-mail: mezher69@uomustansiriyah.edu.iq***

Abstract:

Quantum technology offers new computational, communication, simulation, and metrology methods. Traditional computers need help to solve significant problems like factorization due to exponential increases in computation time. However, quantum computers utilize quantum mechanics for sub-exponential problem size and can simulate nature at the quantum level. Scientists are increasingly interested in developing quantum computers using single ionized atoms in Paul traps. Each ion's ground state represents the least possible qubit value. The 40Ca+ trapped ions were used in a study as an example of a quantum qubit. The MATLAB program was applied to model factors impacting the restricted state and their effects. The solutions must be stable in both directions, requiring three-dimensional confinement of Mathieu's equation. The parameter influences the electrode's distance from the trap center, U_{DC} voltage, ion mass, and radio frequencies. A variable voltage was used to control and demonstrate its impact on a specific chain of trapped ions. This research aims to understand better optimal conditions for confinement and ions' movement from state (4S1/2) to state (4P1/2) by resonance. The quantum state is subject to modification and alteration, making it a promising tool for solving complex problems.

The keywords

(Linear ions trap, Mathieu's equation, the Paul trap, Micromotion, Secular monition (slow harmonic motion)

1. Introduction

Quantum computers can use artificial microstructures, photons, or atoms as components for transforming and storing data [1]. These gadgets have the potential to do computations that were formerly considered to be unachievable in the near future. Controlling trapped ions is the key to successful quantum computing. Scientists have found that ions provide a convenient medium for storing and transmitting data. No major roadblocks are expected to emerge in the pursuit of perfecting trapped-ion computers [2]. Ions retained in ion traps make ideal study models for several physics-related

fields. The precise analysis of the energies and frequency of the ion transitions and the skillfully planned manipulation of quantum states are examples of these fields. Linear Paul traps have gained popularity in recent years for various experiments, studying coulomb force structures and determining the durations of the long-lived metastable excitation states of ions. Additionally, efforts to build quantum computing techniques and the creation of atomic clock domains involve microwave and optical precision hyperfine measurements. Some of these studies give little consideration to the characteristics of the ions' mobility and potential for trapping, treating the trap as little more than a holding chamber for the ions. In contrast, it is frequently required to use ion cooling to reach the lowest temperatures [3]. Ions are arranged in a straight line in a linear Paul trap. The distances between the ions must match the laser beams aim's range, ions can be individually stimulated by lasers and by using a camera to enable excellent resolution detection of fluorescence [4]. As shown in Fig. 1 [5].
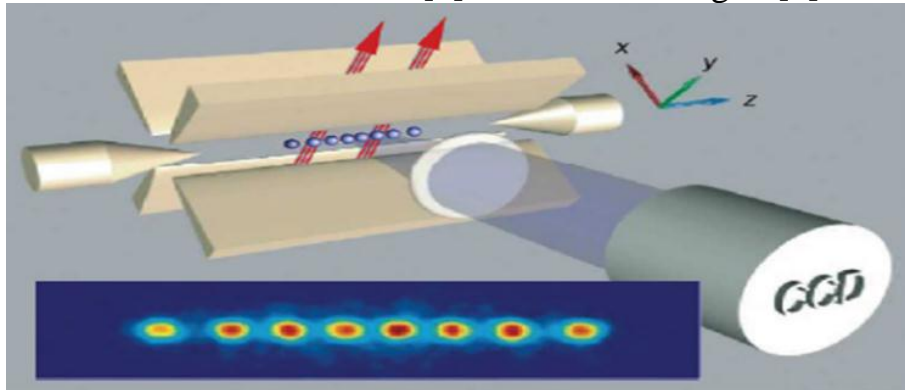

Figure 1 Ions in a straight line in a Paul trap

A combination of U_{DC} (Source for direct current) and radio-frequency voltages are applied to the electrodes in the Paul trap [6]. The solutions of the Mathieu differential formulas illustrating the mobility of an ion within this trap can be either stable or unstable depending on the operating conditions. Other significant amplitude, fundamentally unstable ions crash into the trap or are squandered. A specific **m/e** range of ions can be contained by altering these parameters, where **m** is the ion's mass and **e** is its charge [7]. Ion movement in radio frequency (RF) traps can be explained by driven, secular, and slow harmonic motion, which happens quickly when an electric field is used and is known as micromotion. The excessive Micromotion-induced interaction of the laser light with the ions exhibits a considerable frequency variation. It may reduce the efficiency of quantum logic gates and laser

cooling [8]. Furthermore, second-order Doppler shifts brought on by micromotion may harm trapped ion clocks. Therefore, superior technologies must be able to recognize, track, and consider too much micromotion [9]. Examples include quantum computers and frequency standards. In edge ion trap devices, micromotion detection and compensation are crucial. Since they are denser and closer to the trap surfaces vulnerable to errant U_{DC} electric fields, this can produce excessive micromotion and move the trapping location away from the RF null [6].

2. The theoretical part

Paul traps have a variety of uses, including fundamental quantum physics research, quantum computers, and precision measurements. They are also an essential source for understanding and controlling the quantum state of ions by using trap designs that produce an electric potential (Φ) with a roughly quadrupolar spatial form in the middle of the trapping region. It is also believed that the potential can be divided into a time-dependent part that fluctuates sinusoidally at the rf-drive frequency (Ω) and a time-independent static part. A Paul trap in its ideal form as a fixed component and oscillating electric potential ($U_0 + V_0\ cos\Omega t$) is positioned amid the ring and the two end-cap electrodes. A form's potential is generated by it [10].

$$\Phi\ =\ \frac{U_0 + V_0\ cos\Omega t}{2d^2}(\rho^2\ -\ 2z^2) \cdots\cdots\cdots (1)$$

Where (U_0) the amplitude of the static voltage, (V_0) the amplitude of the sinusoidal voltage, (ρ) the radial distance, (z) the z- direction, and (d) the distance from the trap center to an end-cap electrode.

The trap's centre may be described in three dimensions in terms of the temporal force by carefully tuning the region's amplitude and frequency. That's important for trapping since the particle still flows in both convergent and divergent paths while the electric field alternates. If the equation of motion is solved for an ion of mass **M** and charge **Q** in a Paul field, the conditions of safe confinement for this ion are obtained [11].

$$\frac{d^2u_i}{dt^2} = \frac{Q}{Md^2}(U_0 + V_0\ cos\Omega t)u_i\ , \qquad where\ i = x,y,z \cdots\cdots\cdots (2)$$

Where ($i = x, y, z$) the Cartesian axes.

This creates a homogeneous system of three Mathieu-type differential equations using dimensionless parameters [10].

$$a_x = a_y = -2a_z = -4QU_0/(Md^2\Omega^2)\cdots\cdots\cdots (3)$$
$$q_x = q_y = 2q_z = 2Q\,V_0/(Md^2\Omega^2)\ \cdots\cdots\cdots (4)$$

$$\frac{d^2 u_i}{d\tau^2} + (a_i - 2q_i \cos 2\tau)u_i = 0 \cdots\cdots (5) \qquad \text{where}$$

$$\tau = \Omega t/2 \cdots\cdots (6)$$

The values of (a_i *and* q_i), addressed by the solutions concurrently stable for both directions, agree with the apparent condition for a three-dimensional constraint ($a_z = -2a_r, q_z = 2q_r$). Along a challenging graph, plot the stability limits for both axes as follows: Overlapping zones result in stresses in three dimensions (Fig. 2) [6], [10]. Practically speaking, having a static location near to the source only used for ion trapping is essential [12].
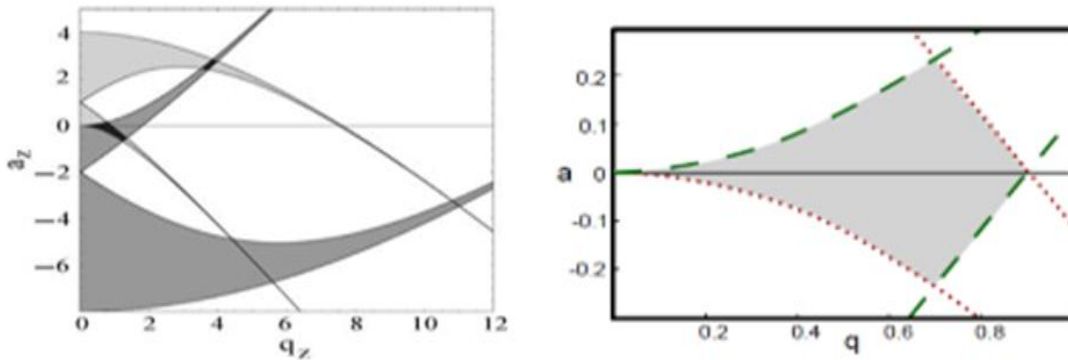

Figure 2 A linear Paul trap's minor stability area represented by black area.

Since the Fourier series may be used to represent the stable Mathieu equation solutions, [13]

$$u_i(\tau) = A_i \sum_{n=-\infty}^{\infty} \varsigma_{2n}\cos(\beta_i + 2n)\tau + B_i \sum_{n=-\infty}^{\infty} \varsigma_{2n}\sin(\beta_i + 2n)\tau \cdots\cdots (7)$$

Where A_i and B_i depending on the starting conditions, remain stable. The stability parameter β_i comprises the functions of (a_i and q_i). The movements of the particle. The amplitudes of the Fourier components, denoted by the coefficients ς_{2n}, decrease as **n** rises. When $a_i, q_i \ll 1$ is small, it's possible roughly approximate the stability value β_i by

$$\beta_i^2 \simeq a_i + \frac{q_i^2}{2} \quad , i = \rho, z \cdots\cdots (8)$$

When using this supposedly adiabatic approximation, only the coefficients ς_{2n} with $n = 1$ supplying $\varsigma_{-2} = \varsigma_{+2} = -(q_i/4)\varsigma_0$ are considered, while the remaining coefficients with $n \geq 2$ are omitted. Ion motion can be minimized to [13].

$$u_i(t) = A_i \left(1 - \frac{q_i}{2} cos\Omega t\right) cosw_i t \quad \cdots\cdots\cdots (9)$$

$$\text{With} \quad w_i = \left(\frac{\beta_i}{2}\right)\Omega \quad \cdots\cdots\cdots (10)$$

That might be thought of as the motion of a frequency oscillator ω for the trap, the amplitude of which is changed at the driving frequency **Ω**. Since the ($\beta \ll 1$) oscillates in **ω**, also known as secular motion or macro motion, it is expected to be slower than the fast micro motion overlaid in **Ω**. The ion motion can be easily divided into two parts because of the stark difference between the frequencies **ω** and **Ω**. While averaging over the frequency of the rapid oscillation, behaviors appropriate for slow motion at that frequency can be viewed as distinct [14].

The parameters (**β_x** and **β_y**) of a two-demotion quadrupole device are only identical up to a specific point; moreover, any parameter other than zero will divide them correspondingly, see (Fig. 3) [14]. The **x** and **y** dimensions experience various secular frequencies. Typically, both electrodes were subjected to a negative **U_{DC}** voltage of **-1V** to achieve this operation [15].

To construct one-dimensional atom chains for use in quantum computers, the radial trapping frequency is chosen to be much greater than the axial frequency. Additionally, suppose one wishes to perform quantum information processing on a single ion using focused laser light. In that case, the separation between the ions in an ion string must be higher than the addressing beam's waist to avert simultaneously addressing multiple ions.
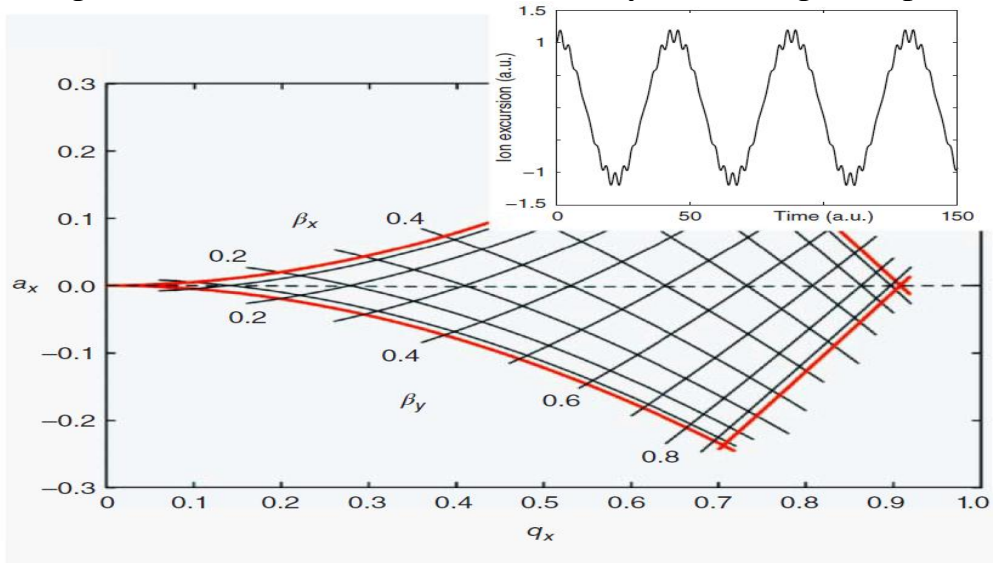

Figure 3 Here is a diagram showing that the linear quadrupole layout is rock solid. The ion route is confined to the volume of the trap within the

red lines. As the solution to the Mathieu equation, the ion's route is shown vs time. $a_x = 0$ and $q_x = 0.2$.

Ions trapped in a vacuum have quantum bits of information stored in their electrical charge states. Since ions are charged particles that may be captured, the trap can use the proper voltages on the entrance electrodes to provide the necessary electric fields for capturing the ions. Harmonic confinement is achieved by the (U_{DC}) gate electrodes in the **z**-direction, while an effective harmonic potential is generated by the Four electrodes in the **x-y** plane. There is a great deal of eigenstates for the potential of a harmonic oscillator. Ions are laser-cooled to their vibratory ground state to stop them from being randomly excited to higher energy levels due to temperature effects and fluctuating electromagnetic fields. The ions will be aligned in a chain along the **z**-axis to counteract the force created by their Coulomb interaction with the help of the external forces [16].

Since the micromotion disappears for all ions along the **z**-axis, this strategy is very useful for a three-dimensional Paul trap. The direction of oscillation is also determined arbitrarily and independently of the radial secular frequency. In contrast, ions experience micromotion heating owing to Coulomb repulsion when confined in three-dimensional Paul traps. It is said that even for long chains of ions, linear Paul traps are able to deplete this heating source. Therefore, a modified version of the three-dimensional Paul trap has been used to create strings of two and three ions. However, it seems preferable to use linear traps for larger amounts of ions [17].

3.   The theoretical work

The main elements of the MATLAB simulation method are shown in (Fig. 4), which also demonstrates how calculations were performed and the results were compared to experimental results.
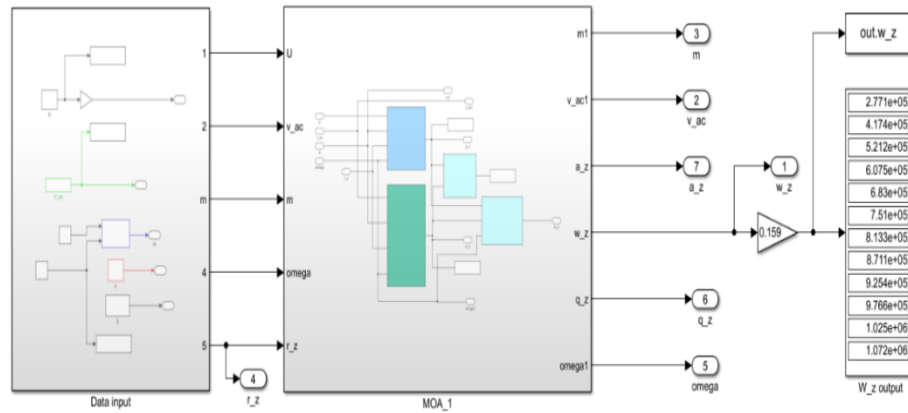
Figure 4 A diagram showing the simulation process performed in the MATLAB program.

Our ion trap is made of four segmented copper rods with a diameter of $5\ mm$. The closest distance from the center is $1.1\ mm$ at r_0. The distance between the end-cap electrodes and the trap center z_0 is $2.5\ mm$. A radio frequency field with a frequency of $\Omega/2\pi = 11.2\ \text{MHz}$ and variable amplitude operates the trap. We select **900 V** for $\mathbf{V_{AC}}$, and a voltage $\mathbf{U_{DC}}$ in range of **0** to **220 V** is applied to the end caps about the center segments to achieve axial confinement. The trap is housed in a vacuum tank with a $10^{-10}\ mbar$ base pressure. In our study, ion **40Ca+** was used. Ions are created within the trapping chamber by electro-ionizing an atomic beam. The trap electrodes have been carefully guarded against contamination with neutral **Ca** since doing so would lead to faults in the trapping field via contact potentials.

The $4S_{1/2} - 4P_{1/2}$ resonance transition of **40Ca+** at **397 nm** is excited by light from a frequency-doubled laser, which causes fluorescence to be observed at the same wavelength. To avoid trapping ions in the long-lived metastable $3D_{3/2}$ state, into which the excited $4P_{1/2}$ state may decay, we used a diode laser at **866 nm** that was resonance tuned to this transition for repumping. Along the **z**-axis, the two lasers overlapped and pointed into the trap. Both lasers are protected against frequency drift. To modify the effective linewidth of the long-lived optical transition, the excited state lifetime must be purposefully reduced during cooling. The population is pumped from the $3D_{5/2}$ state to the $4P_{1/2}$ state via the $4P_{3/2}$ level using light at an **854 nm** wavelength (Fig. 5) [18].
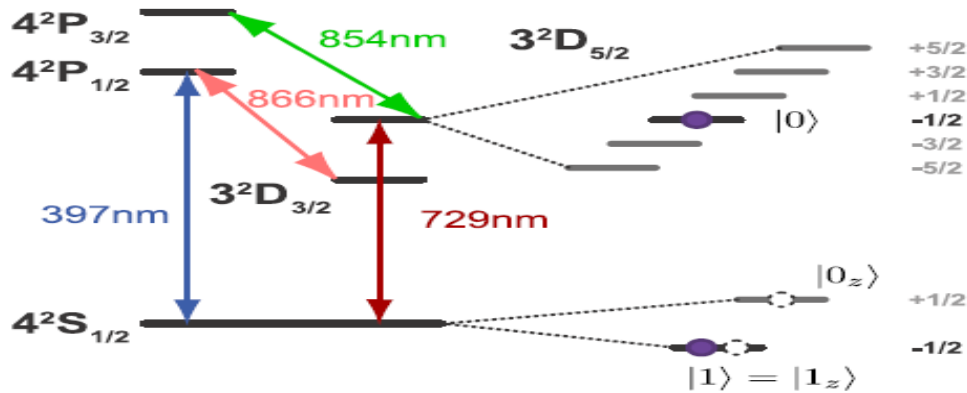
Figure 5 The 40Ca+ leveling system. Conventional photonic qubits $(4S_{1/2}(m_j = -1/2) = |1\rangle)$ **and** $(3D_{5/2}(m_j = -1/2) = |0\rangle)$ **which are displayed as solid circles. The ground state qubits are shown as open circles.** $(4S_{1/2}(m_j = -1/2) = |1\rangle z)$ **and** $(4S_{1/2}(m_j = 1/2) = |0\rangle z)$**, that are resistant to spontaneous decay.**

The simulation technique was used to compare the impacts of each axial confinement for a separate band of ions. Select a group of ions between **2** and **10**, to begin with inside the confinement space. That falls inside the permitted range for the voltage U_{DC} we selected for axial confinement. The Mathieu equation can be solved to determine that each coefficient (a_i, q_i) will significantly affect how these ions flow. Where (a_z, q_z) and (a_r, q_r) stood for the axially and radially confinement coefficients, respectively. This program allowed for the tracking of that motion. The right place for the resonance frequency that matched the used frequency was selected for each case collected. We obtain the coefficients $a_r \approx 0.28$ and $q_r \approx 0.72$ for V_{AC} voltage at **900 V**, respectively. The radial confinement is stable as long as (q_r) is minor than approximately **0.9** [19]. Due to the set V_{AC} voltage value, these coefficients remain constant. While the coefficients (a_z, a_r) will have different values, as given in the following table.

Table 1 The resalt from our program.

U_{Dc} (V)	a_z	W_z (MHz)	a_r	W_r (MHz)
0	0	1.9243	0	2.8625
20	0.0022	3.2356	0.0322	3.0333
40	0.0043	4.1516	0.0643	3.1949
60	0.0065	4.8992	0.0965	3.3487
80	0.0086	5.5470	0.1286	3.4958
100	0.0108	6.1266	0.1608	3.6369
120	0.0130	6.6559	0.1930	3.7728
140	0.0151	7.1462	0.2251	3.9039
160	0.0173	7.6049	0.2573	4.0307
180	0.0195	8.0375	0.2894	4.1537
200	0.0216	8.4479	0.3216	4.2732
220	0.0238	8.8393	0.3538	4.3894

Figure **6** depicts ion motion under various operational circumstances, and this study exhibits both secular and minute movements for each situation of (a_z, a_r) that we obtain. Figures 7 and 8 show ion motion along the Z-axis. While Figures **9** and **10** illustrate the ion trend along the radial direction, that also covers the axes (**X** and **Y**).
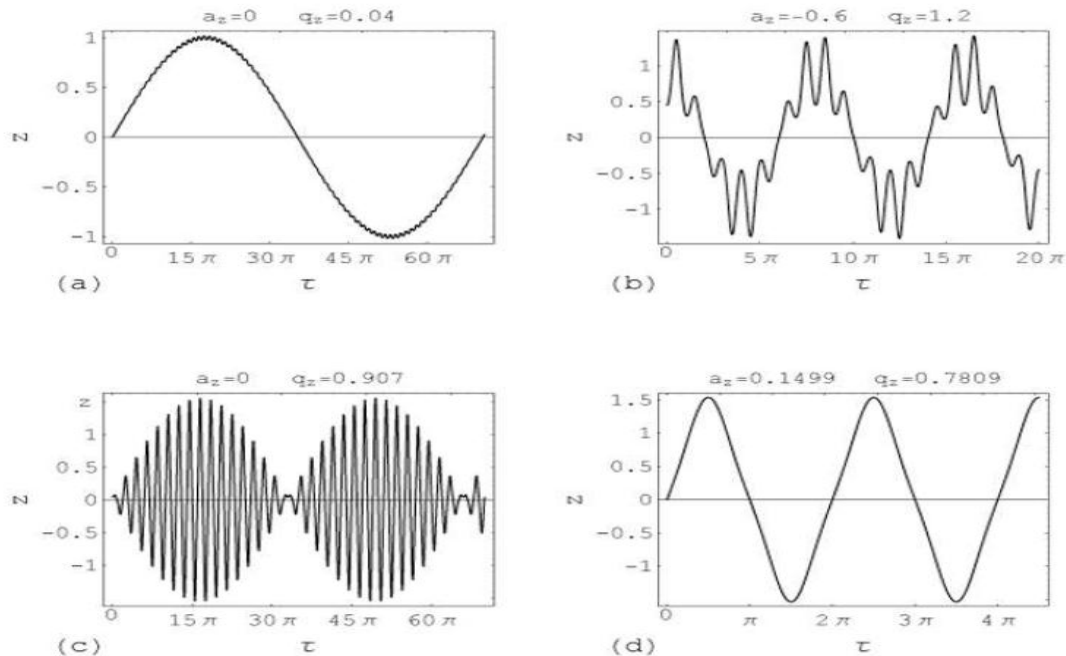

Figure 6 Ion motion under various operating circumstances [20].
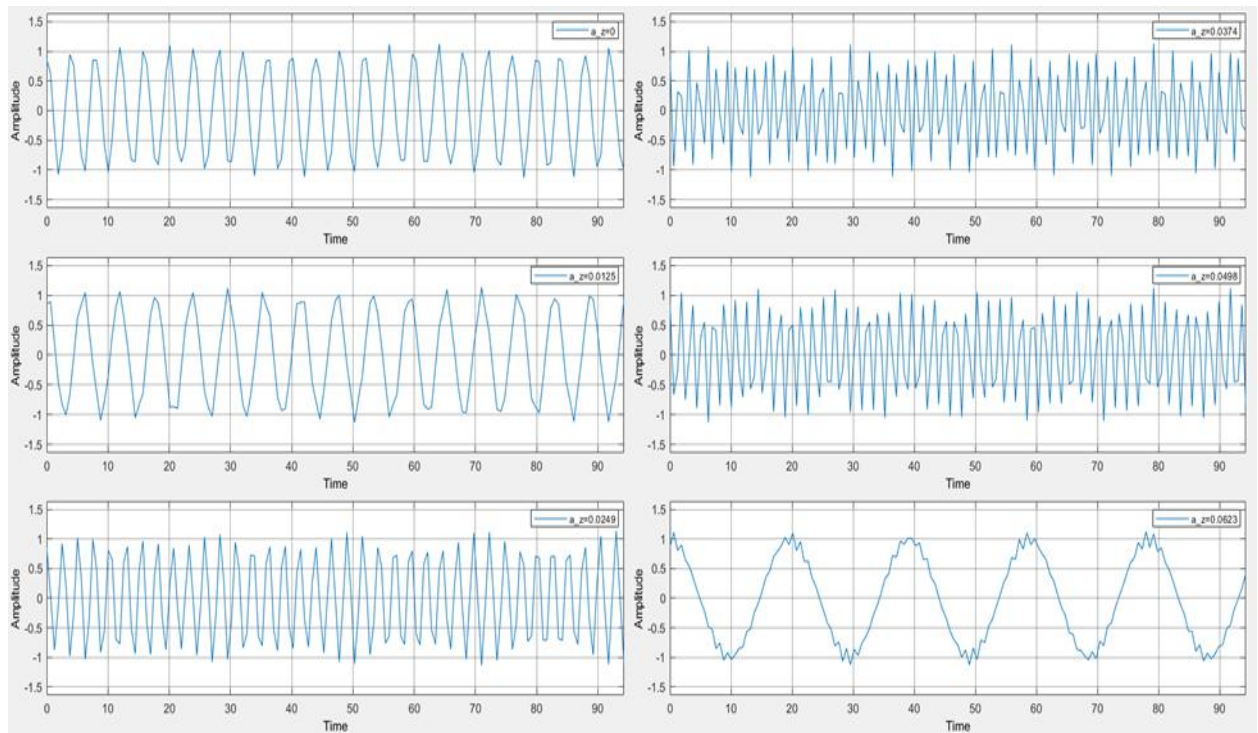
Figure 7 Ionic motion along the axis of the Z-axis at
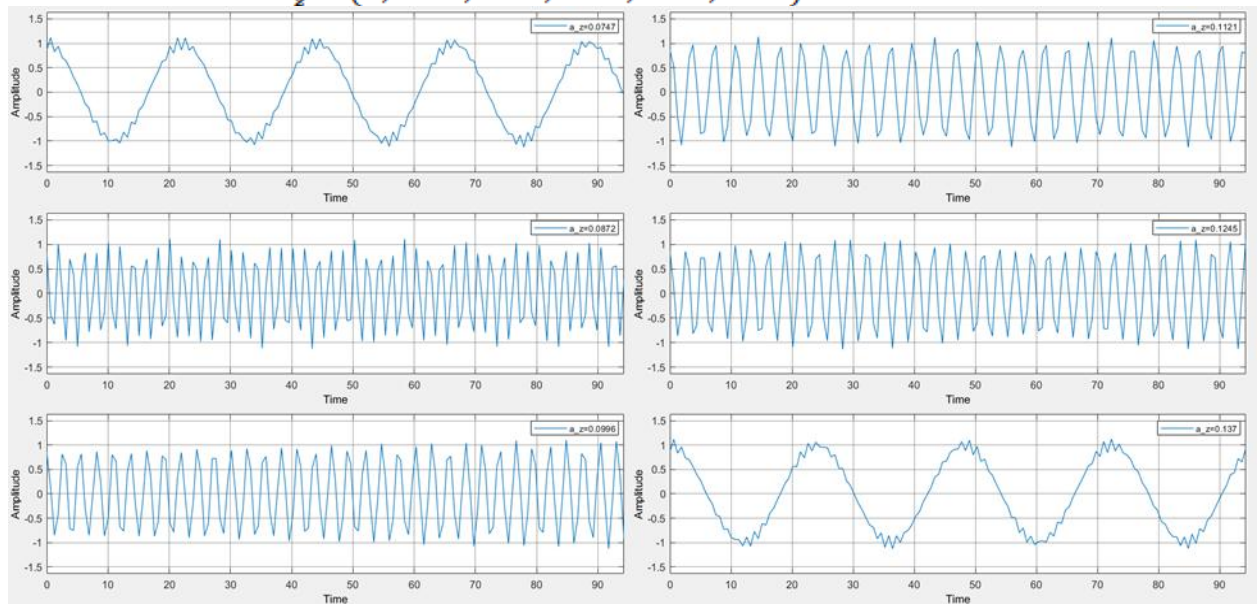$$a_z \approx (0, 1.25, 2.49, 3.74, 4.98, 6.23) \times 10^{-2}$$

Figure 8 Ionic motion along the axis of the Z-axis at
$$a_z \approx (7.47, 8.72, 9.96, 11.21, 12.45, 13.7) \times 10^{-2}$$
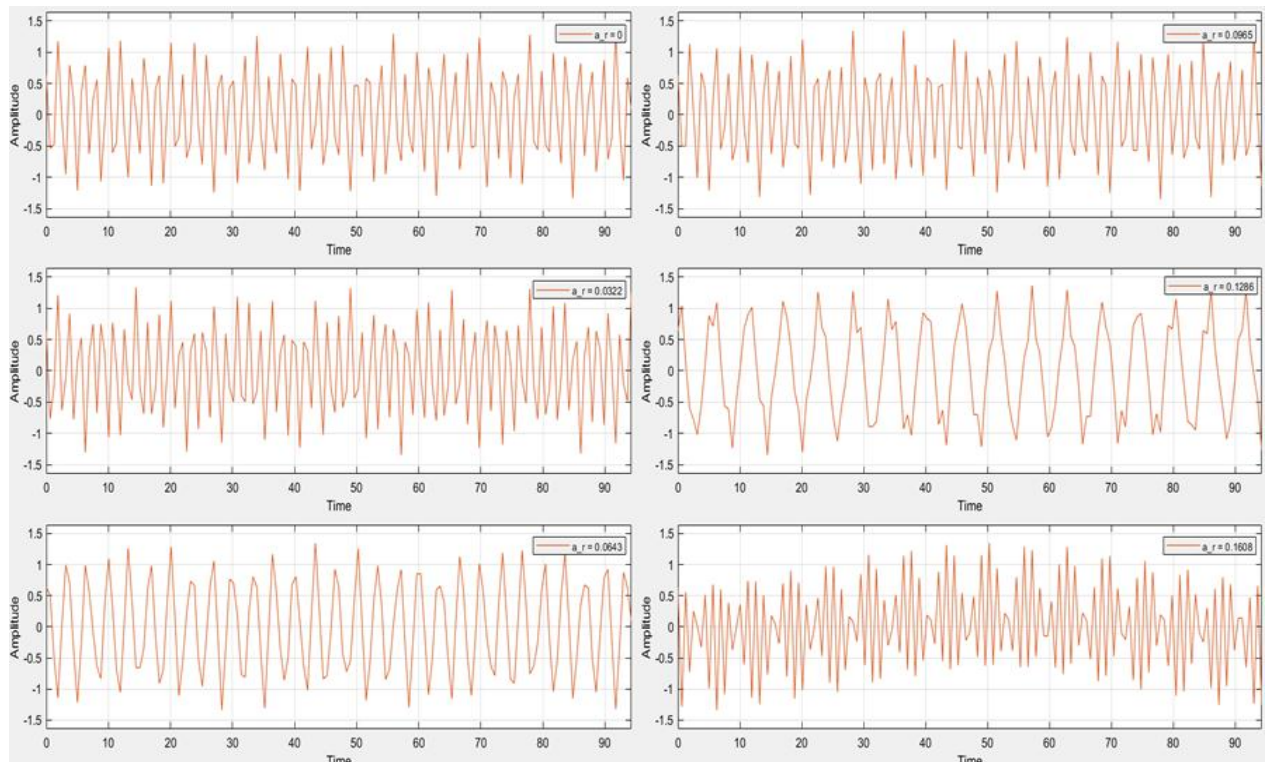
Figure 9 The movement of ions in the radial direction at
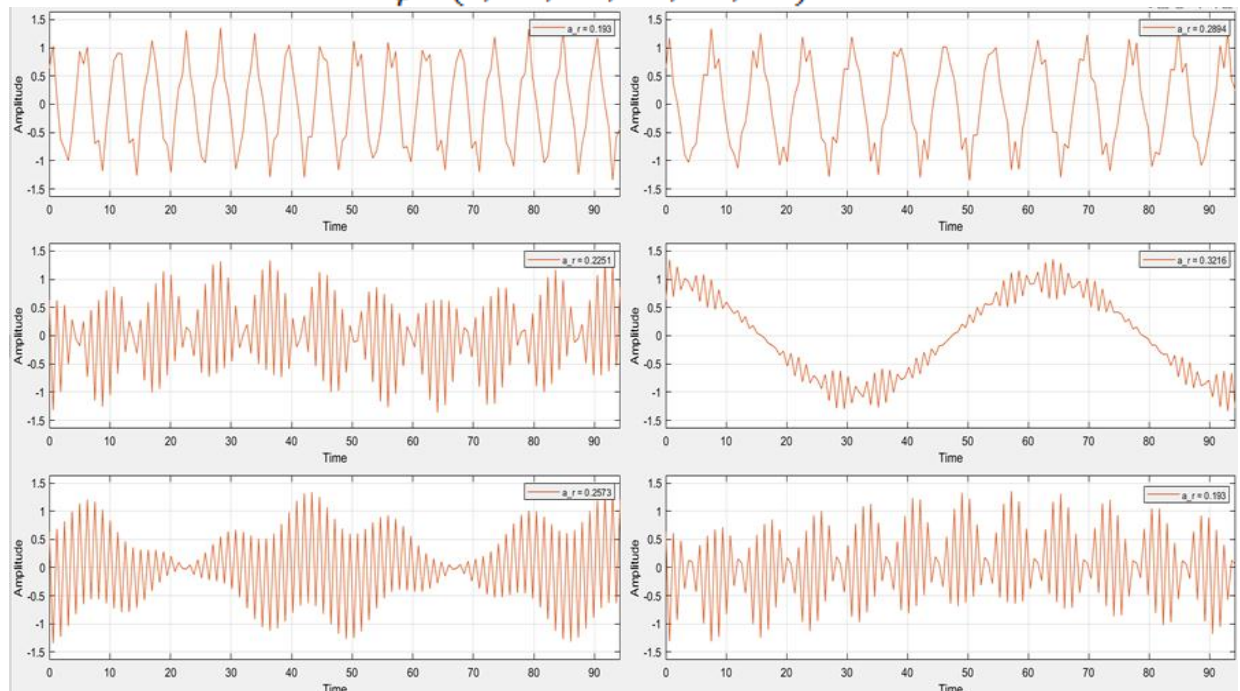
$$a_r \approx (0, 0.3, 0.6, 0.9, 1.2, 1.5)$$

Figure 10 The movement of ions in the radial direction at

$$a_r \approx (1.8, 2.1, 2.4, 2.7, 3, 3.3)$$

The diagram in (Fig.**11**) depicts the U_{DC} voltage with ion distance to increase the number of ions trapped inside the confinement region.
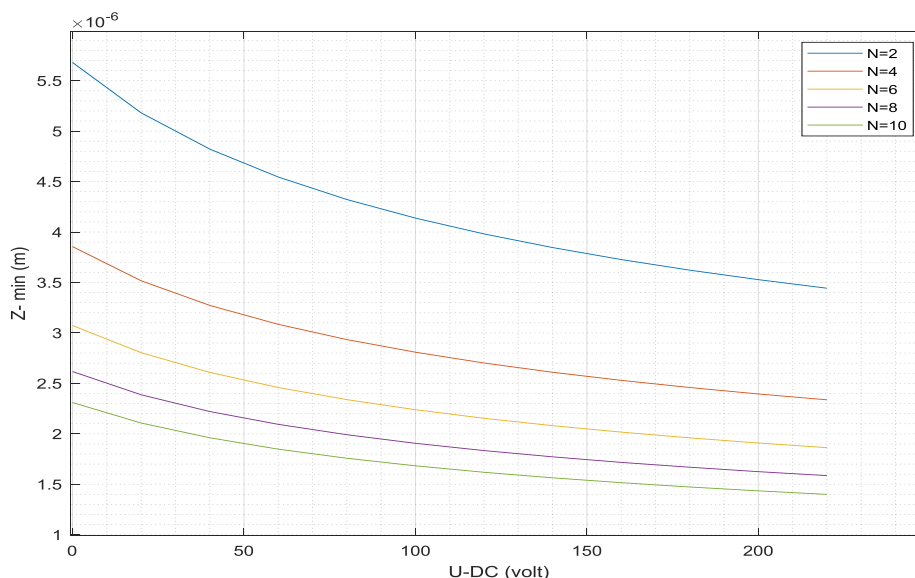

Figure 11 The relationship between the minimum distance between ions and U_{DC} voltage.

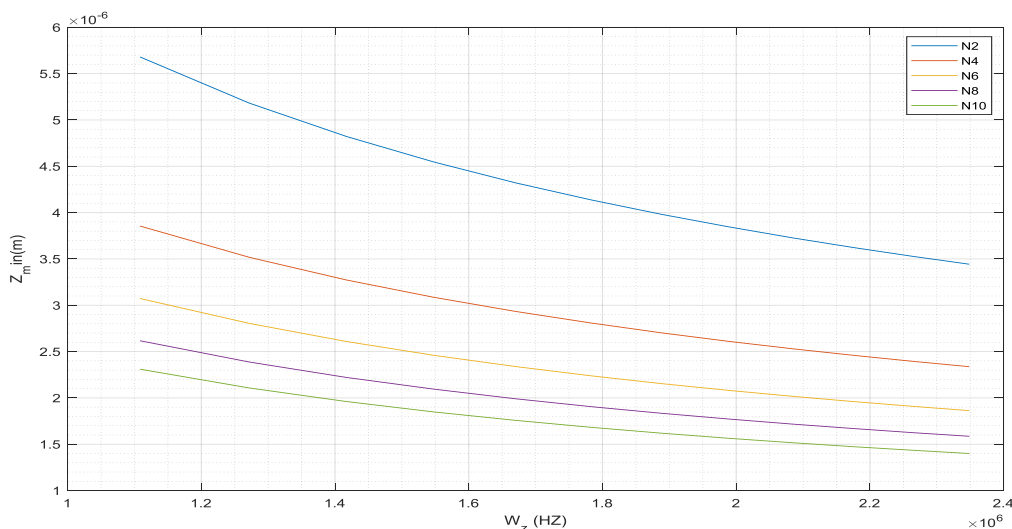In Figure.12, it is demonstrated how axial oscillation frequencies relate to ion distance.

Figure 12 The relationship between the minimum distance between ions and the axial frequency (W_z).

4. The discussion

The table shows that different values of (a_z and a_r) have a big influence on the axial frequency (W_z) and radial frequency (W_r), respectively. Knowing each of (W_z and W_r) is one of the most important effects for users who want to build a quantum computer using ions that have been trapped. The relationship $N_{max} = 1.82(Wr/Wz)^{1.13}$ is used to calculate the most ions that can fit inside the space of a linear design. [21]

The experiment only included five ions, for starters. Increasing the confining zone's capacity to hold ions requires adjusting the axial frequency. One method is to separate the center electrode from the end caps by 5 mm. Our inquiry will get to that point now.

Second, the quantity of the Coulomb force between the ions and the diameter of the laser pulse used for cooling and exciting the ions are both dependent on the distance between the ions. According to Table (1), we observed this for two different ions. As the secular frequency rises, the ions' distance from one another decreases, which has a negative impact on the confinement process. It will be more difficult to exert control over the ion by means of the laser pulse for cooling or pumping if the Colome force between the ions is stronger. Since a single ion is all that the diameter of the laser pulse can reach, the largest possible gap is chosen.

Where (Fig.11) depicts how the ion separation distance will shrink as the U_{DC} voltage rises. Additionally, when the quantity of ions rises, the available distance will similarly contract. This distance can be altered when a low **DC** voltage is applied.

Figure 12 displays the connection between axial frequency and ion separation. Because raising the U_{DC} voltage also increases the axial frequency, this confirms the previous relationship. Additionally, it provides a connection $\Delta Z_{cm} = \sqrt{\hbar/2NmW_z}$) that shows how to calculate the center of mass coordinate, which should be lesser than the separation among ions, particularly when utilizing various laser beams. [14]

Finally, it influences how the Lamb-Dicke factor (μ) is calculated. This element controls the amount of momentum transferred from the ions to the optical field. For a single ion and coupling to a single vibrational mode, this is determined by the ratio of the wavelength of the driving radiation to the position-space ground-state wave function of the ion.[10]

5. Conclusion

Controlling inside the confinement region requires the ions to function appropriately through quantum manipulation techniques. Control of these ions is affected by factors such as the ions' mass, the trap's geometrical characteristics, and the electrodes' operating mode. The assessment procedure is directly affected by each of these factors. In this analysis, we looked at how the total amount of U_{DC} voltage affects the limiting factor. We stated that there must be some slight influence on the ions' motion to increase confidence in their ability to be contained within a constrained and stable region.

In addition, the U_{DC} voltage guarantees that the ions are carried in a straight path and handled as a series. Accelerating the ion-to-ion vibration process and, by extension, the heat created by this vibration, the quadrupole's Ac voltage induces the movement of the ions in the confined zone. As a result, the continuous effort dampens these vibrations and severely limits their freedom of movement. The solution to Matthew's equation and the depiction of the amplitude and velocity of the vibrating ions makes this abundantly clear. Raising the ion density inside the confinement zone is discussed, along with the results. As the quantity of ions rises, so does the difficulty of the control mechanism. Consequently, while using a fixed number of ions to fabricate quantum qubits, it is important to choose a voltage that is suitable for the task. All of this was handled by MATLAB's simulation programme.

Reference

[1] E. Knill, "Quantum computing," *Nature*, vol. 463, no. 7280, pp. 441–443, 2010.

[2] S. Resch and U. R. Karpuzcu, "Quantum computing: an overview across the system stack," *arXiv preprint arXiv:1905.07240*, 2019.

[3] J. C. Bardin, D. H. Slichter, and D. J. Reilly, "Microwaves in quantum computing," *IEEE journal of microwaves*, vol. 1, no. 1, pp. 403–427, 2021.

[4] T. Feldker *et al.*, "Rydberg Excitation of a Single Trapped Ion," *Phys Rev Lett*, vol. 115, no. 17, Oct. 2015, doi: 10.1103/PhysRevLett.115.173001.

[5] R. Blatt and D. Wineland, "Entangled states of trapped atomic ions," *Nature*, vol. 453, no. 7198, pp. 1008–1015, 2008.

[6] L. A. Zhukas, M. J. Millican, P. Svihra, A. Nomerotski, and B. B. Blinov, "Direct observation of ion micromotion in a linear Paul trap," *Phys Rev A (Coll Park)*, vol. 103, no. 2, p. 023105, 2021.

[7] M. B. Quadrelli and P. Ius, "Modeling and simulation of trapping mechanisms of granular media in space," in *AIAA/AAS Astrodynamics Specialist Conference*, 2016, p. 5572.

[8] R. C. Thompson, "Ion coulomb crystals," *Contemp Phys*, vol. 56, no. 1, pp. 63–79, 2015.

[9] T. F. Gloger *et al.*, "Ion-trajectory analysis for micromotion minimization and the measurement of small forces," *Phys Rev A (Coll Park)*, vol. 92, no. 4, p. 043421, 2015.

[10]   M. Knoop, I. Marzoli, and G. Morigi, *Ion Traps for Tomorrow's Applications*, vol. 189. IOS Press, 2015.

[11]   T. W. Penny, "A Low-Noise Electrically Levitated Oscillator for Investigating Fundamental Physics," University College London, 2022.

[12]   K. Singer *et al.*, "Colloquium: Trapped ions as quantum bits: Essential numerical tools," *Rev Mod Phys*, vol. 82, no. 3, p. 2609, 2010.

[13]   K. A. Brown and T. Roser, "Towards storage rings as quantum computers," *Physical Review Accelerators and Beams*, vol. 23, no. 5, p. 054701, 2020.

[14]   F. Schmidt-Kaler and U. Poschinger, "Quantum Computing Experiments with Cold Trapped Ions," *Quantum Information: From Foundations to Quantum Technology Applications*, pp. 519–551, 2016.

[15]   M. Wang, "Halo Ion Trap Mass Spectrometry: Design, Instrumentation, and Halo Ion Trap Mass Spectrometry: Design, Instrumentation, and Performance Performance," 2010. [Online]. Available: https://scholarsarchive.byu.edu/etd

[16]   T. S. Humble, H. Thapliyal, E. Munoz-Coreas, F. A. Mohiyaddin, and R. S. Bennink, "Quantum computing circuits and devices," *IEEE Des Test*, vol. 36, no. 3, pp. 69–94, 2019.

[17]   P. Blanchard, D. Giulini, E. Joos, C. Kiefer, and I.-O. Stamatescu, "Decoherence: Theoretical, Experimental, and Conceptual Problems: Proceedings of a Workshop Held at Bielefeld Germany, 10–14 November 1998," 2000.

[18]   P. Schindler *et al.*, "A quantum information processor with trapped ions," *New J Phys*, vol. 15, Dec. 2013, doi: 10.1088/1367-2630/15/12/123012.

[19]   D. T. Snyder, W.-P. Peng, and R. G. Cooks, "Resonance methods in quadrupole ion traps," *Chem Phys Lett*, vol. 668, pp. 69–89, 2017.

[20]   G. Werth, "Basics of ion traps," *Lecture notes*.

[21]   W. Lange, "Quantum Computing with Trapped Ions." 2009.

منطقة الاستقرار المحصورة في مصيدة باولي الخطية لأيونات Ca+40

مزهر باقر صالح [(2)]

كلية العلوم الجامعة المستنصرية / قسم الفيزياء
07726904802

باسم رحيم كاظم [(1)]

كلية العلوم الجامعة المستنصرية / قسم الفيزياء
مديرية تربية كربلاء
07709650553

mezher69@uomustansiriyah.edu.iq   *basemraheem@uomustansiriyah.edu.iq*

مستخلص البحث:

تقدم تكنولوجيا الكم طرقًا حسابية واتصالات ومحاكاة وقياسًا جديدة. تحتاج أجهزة الكمبيوتر التقليدية إلى المساعدة في حل المشكلات المهمة مثل التحليل بسبب الزيادات الهائلة في وقت الحساب. ومع ذلك، تستخدم أجهزة الكمبيوتر الكمومية ميكانيكا الكم لحجم المشكلة الأسي الفرعي ويمكنها محاكاة الطبيعة على المستوى الكمي. يهتم العلماء بشكل متزايد بتطوير أجهزة الكمبيوتر الكمومية باستخدام ذرات متأينة مفردة في مصائد باولي. تمثل الحالة الأساسية لكل أيون أقل قيمة ممكنة للبت الكمي. تم استخدام الأيونات المحتجزة **Ca40+** في إحدى الدراسات كمثال على الكيوبت الكمومي. تم استخدام برنامج MATLAB على العوامل النموذجية التي تؤثر على الحالة المقيدة وتأثيراتها. يجب أن تكون الحلول مستقرة في كلا الاتجاهين، مما يتطلب حصرًا ثلاثي الأبعاد لمعادلة ماثيو. تؤثر المتغيرات على المسافة من مركز المصيدة لنهاية القطب، وجهد **U_{DC}**، وكتلة الأيون، والترددات الراديوية. تم استخدام جهد متغير للتحكم وإظهار تأثيره على سلسلة محددة من الأيونات المحاصرة. يهدف هذا البحث إلى فهم أفضل للظروف المثلى للحجز وحركة الأيونات من الحالة (**4S_{1/2}**) إلى الحالة (**4P_{1/2}**) بالرنين. تخضع الحالة الكمومية للتعديل والتغيير، مما يجعلها أداة واعدة لحل المشكلات المعقدة.

الكلمات المفتاحية: فخ الايونات الخطية، معادلة ماثيو، الحركة الدقيقة، الحركة العلمانية (الحركة التوافقية البطيئة).